Characterization of spatial heterogeneity in groundwater applications

PhD Thesis

Department of Geotechnical Engineering and Geo-Sciences (ETCG)

Technical University of Catalonia, UPC

Paolo Trinchero

February 2009

HYDROGEOLOGY GROUP
TECHNICAL UNIVERSITY OF CATALONIA

Chapter 6

Assessing preferential flow through an unsaturated waste rock pile using spectral analysis*

6.1 Introduction

In most natural soils irregular paths exist where water and solutes move faster bypassing most of the porous matrix. These mechanisms are of great importance in mining related problems where the chemical composition of mine water release depends on the residence time of the water within the medium.

One of the main cause of preferential flow is the high heterogeneity of natural soil textures. These can include (1) macropores generated by cracks or spatial arrangement of well-structured soils [6], (2) earthworms burrows [28] and root channels [37] in unstructured soils, (3) heterogeneity of the granular matrix [71] and (4) textural boundaries that result in horizontal redirection

* Trinchero, P., Beckie, R., Sanchez-Vila, X., Nichol, C. in preparation for submission .

(i.e. funneling) of water [54, 55]. Preferential flow is also attributable to instability of the wetting front that can be either related to the textural structure of the matrix [23] or induced by specific behaviors of the fluids involved [4, 47].

In the last decades several works have documented the existence of preferential flow through the assessment of field evidence. *Roth et al.* [78] analyzed horizontal averaged concentration profiles of chloride that developed after solute was applied at the surface. They observed that the initial pulse of solute split into a main pulse, moving slowly, and a second deeper front (moving quickly). The development of preferential flow mechanisms in a medium having a water repellent topsoil was studied by *Ritsema et al.* [76] who argued that, in these media, water and tracers are horizontally redistributed before finding a preferential flow path. *Flury et al.* [31] studied the flow pathways of water in 14 different soils through the use of dye-tracers. They found that the maximum penetration of water was deeper in structured than in nonstructured soils. Their results also showed that the flowpaths were dependent on the initial soil water content ('wet' or 'dry') although a common model was not found. Observations of the vertical distribution of environmental isotopes (tritium, oxygen 18 and deuterium) demonstrated the existence of preferential flow in the vadose zone of the Negev desert (Israel) [65]. Water discharge and tracer arrival time at different lysimeters located at the bottom of a waste rock pile were studied by *Nichol et al.* [70] to assess the existence of preferential flow. The results of the tracer experiments showed a great spatial variability with some lysimeters having a fast response to the perturbation generated at the surface and others where flow and transport where mainly driven by the matrix.

An extensive body of literature exists that deals with different approaches to model flow in unsaturated structured soils [87, 36]. In these media, the difficulty to apply flow and transport models based on Richards' equation has been overcome by the development of dual-domain approaches that consist in either assuming that flow and transport are restricted to fractures and macropores where the matrix is considered an immobile zone (dual-porosity models) [96] or considering that the rate of flow and transport is different in each zone (dual-permeability models) [35].

The difficulty of implementation of mechanistic models (i.e. dual porosity models) arises from the need of a rigorous microscopic description of the medium to obtain reliable 'upscaled' hydraulic parameters. This description is often infeasible in real applications where the size of the medium and the high heterogeneity of its textural structure make impossible a detailed characterization of its hydraulic properties. An alternative procedure consists in lumping all the parameters together and focusing on the average behavior of the system. The approach that we pursue here assumes the medium is a linear filter and simulates the output of the system (e.g. outflow, concentration, etc.) as the input convoluted with the filter, which is also called a transfer function TF. This methodology has been extensively used in many hydrogeological studies in particular concerning the analysis of spring flow from karst aquifers [26, 59, 24].

In this work we model unsaturated water flow in a complex, highly heterogeneous system using a simple linear representation. The aim of this approach is to identify the average behavior of the system and specifically the mean rate of preferential flow occurring and some characteristic time scale of the flow through the matrix. The model is implemented by computing the empirical TF of lysimeters at the base of Nichol et al's (2005) experimental waste rock pile. The TF is then parametrized by decoupling the two flow components (fast and slow). A similar approach was used by *Molenat et al.* [64] to simulate the response of a catchment to a rainfall event. The fit of the parametric TF with the empirical one allows to estimate the two above-mentioned parameters.

6.2 Study area and monitoring scheme

The data set that we examine here comes from the instrumented waste-rock pile experiment of *Nichol et al.* [70] at the Cluff Lake Uranium Mine in northern Saskatchewan (Canada). The waste rock at the mine is composed of aluminous gneisses and granitoids from the Precambrian Peter River Gneiss formation. Waste rock is defined as any rock that must be removed to gain access to ore-grade material at a mine. The waste rock at the Cluff Lake Mine has a broad grain size

distribution, which included boulders up to 1.5 *m* in diameter. The proportion of fine material ($< 2mm$) was sufficiently large ($> 20\%$) that the waste rock was expected to behave more like a soil than a coarse granular material [88].

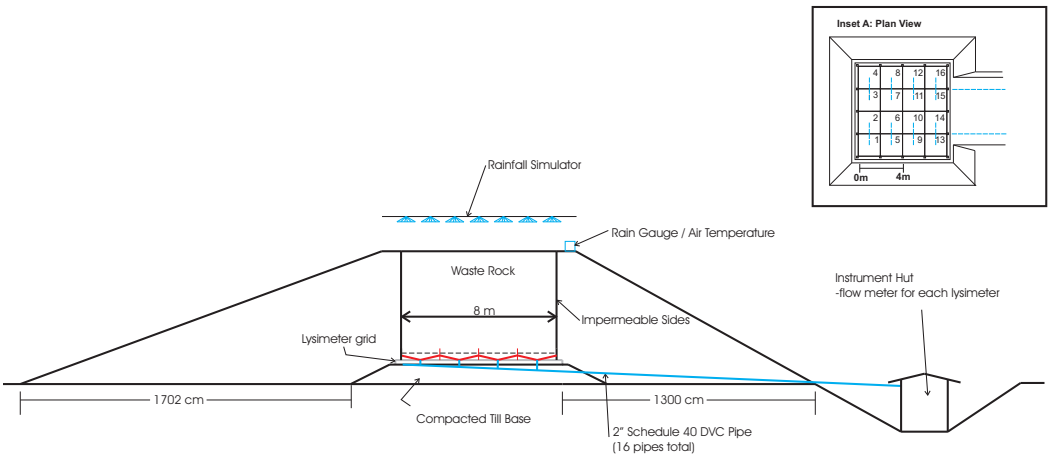

Figure 6.1: Simplified cross section of constructed pile experiment and plan view of experiment core (inset A).

The instrumented experimental waste-rock pile was constructed at the site in 1998 and was designed to mimic the behavior of the upper 5 *m* of a much larger unsaturated waste rock pile. Simplified plan and cross sectional views of the pile are shown in Figure 6.1. The instrumented core of the pile has a footprint of 8 *m* by 8 *m* and is 5 *m* high. Outflow from the base of the pile is collected in a contiguous grid of 16 lysimeters (Figure 6.1, Inset A). This design leads to the formation of a water table at the base of the pile. The pile rests on a contoured cement pad lined with a PVC geomembrane. Plywood lined with a 60 mil HDPE geomembrane was placed from the base of the pile to the surface to isolate the central core of the pile and prevent lateral diversion of flow around the zero pressure lysimeters at the base. The sides provide lateral no-flow boundaries to matrix flow, allowing all flow to be captured at the basal lysimeters but also limit the possible lateral extent of spatially-distinct flow pathways. Waste rock was placed in the pile using a large excavator, taking care to prevent damage to instrumentation. The resulting waste rock texture matches the range of textures seen in excavations of existing waste rock piles on site. It is highly

heterogeneous, ranging from 1.5 m diameter boulders to clay, with areas that are matrix supported and areas with matrix-free cobbles and boulders. Outflow from each 2 m by 2 m lysimeter is separately piped to an instrumentation hut where outflow is measured using tipping-bucket rain gauges. The raw data set consists of the event times of each tip of each rain gauge flow meter. A rain gauge on top of the pile recorded incident natural and artificial rainfall events. Additional information about the setup can be obtained from [70]

6.3 Modeling approach

6.3.1 General overview of the methodology

We use linear systems theory and rainfall and outflow data to identify a non-parametric empirical transfer function. We then fit a model with two parameters to the empirical transfer function to provide a parameterized transfer function model. In linear systems, convolution is used to describe the relationship between three signals: the input signal, X, the impulse response (i.e. the output of a delta function input signal), f, and the output signal, Y. This relationship can be expressed as follows

$$Y(t) = \int_{-\infty}^{\infty} f(t-\tau)X(\tau)d\tau \tag{6.1}$$

According to the spectral representation theorem, a stationary stochastic process X has a spectral representation of the form

$$X(t) = \int_{-\infty}^{\infty} \exp^{i\omega t}\, dZ_X(\omega) \tag{6.2}$$

where $dZ(\omega)$ are the complex Fourier amplitudes of a process with ortogonal increments Z, ω is the frequency and $i = (-1)^{1/2}$ [75].

From the properties of the orthogonal processes it follows that

$$E\left[dZ_X(\omega)dZ_X^*(\omega')\right] = \delta_{ij}\phi_{XX}(\omega)d\omega \tag{6.3}$$

where E [ ] is the expected value, the asterisk denotes the complex conjugate, ϕ_{XX} is the spectral density or spectrum of $X(t)$ and δ_{ij} is the Kronecker delta.

Equation (6.2) and (6.3) allows us to express (6.1) in spectral representation

$$\phi_{YY}(\omega) = |F(\omega)|^2 \phi_{XX}(\omega) \tag{6.4}$$

where $\phi_{YY}(\omega)$ is the spectrum of the output signal and $|F(\omega)|^2$ is the transfer function (TF).

6.3.2 Estimation of the TF

In our work we are concerned about the spectral signature of the water that after infiltrating at the top of the pile is released at the bottom and collected in each lysimeter. The data we use comes from an eight-month period (March 1 to October 31, 2000). During the winter season the top of the pile is frozen and so rainfall does not produce input. Thus, we have not included this part of the time series in our study.

The transfer function is given by the spectrum of the output (i.e. outflow through a given lysimeter) divided by the spectrum of the input (i.e. effective infiltration in the section projected vertically for each given lysimeter) and can be expressed as follows

$$\left|F_{emp}(\omega)\right|^2 = \frac{\phi_{qq}(\omega)}{\mu^2\phi_{rr}(\omega)} \tag{6.5}$$

where $\left|F_{emp}(\omega)\right|^2$ is the empirical transfer function, $\phi_{qq}(\omega)$ and $\phi_{rr}(\omega)$ are the spectra of the

output and input, respectively, and μ is a normalization coefficient.

6.3.3 Data analysis

For the study period, rainfall data consists of a time series of 3221 unevenly spaced tipping-bucket raingauge event times. The effective input (i.e. effective infiltration) is given by the rainfall minus the evapotranspiration (no runoff is observed at the site). Horizontal redistribution also plays an important role within each section of the pile. The normalization coefficient, μ, in (6.5) implicitly accounts for both evapotranspiration and internal water redistribution and is calculated as the ratio of the water released by the given lysimeter divided by the volume of precipitation for the given section during the period considered (see Table 6.1). The average value of $\mu = 0.63$ indicates that 37% of rainfall does not reach the lysimeters, which we associate to evapotranspiration. The fact that two lysimeters (lysimeter 6 and 13) have a μ larger than 1 is indicative of the importance of horizontal redistribution in these kinds of media as already observed by [76].

To reduce numerical leakage, before computing the periodogram each series has been tapered using a cosine bell taper. Then the spectrum has been estimated by mean of the periodogram computed using the Lomb algorithm [58].

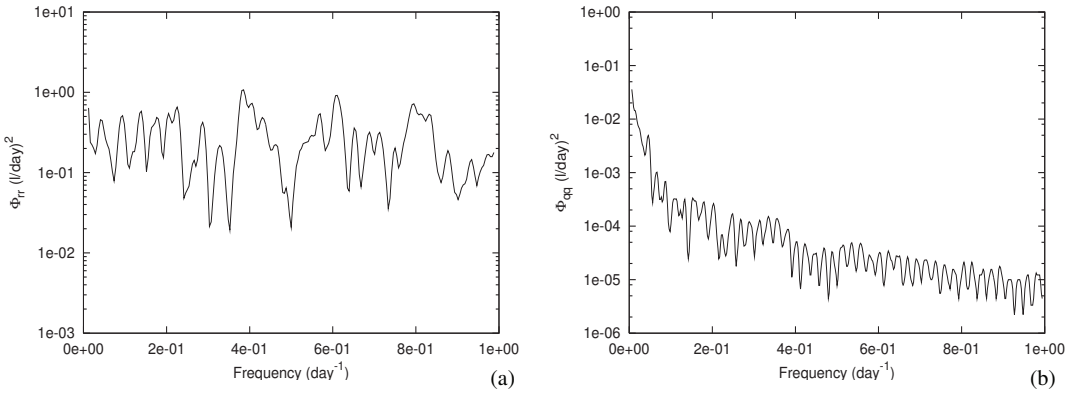

Figure 6.2: Periodogram of the rainfall (a) and of the outflow through lysimeter 9 (b).

lysimeter number	water released (m^3)	μ
1	0.68	0.53
2	0.77	0.60
3	0.39	0.30
4	0.62	0.48
5	0.44	0.34
6	2.01	1.56
7	0.82	0.64
8	0.57	0.44
9	0.56	0.43
10	0.86	0.67
11	0.89	0.69
12	0.71	0.55
13	1.37	1.06
14	0.82	0.64
15	0.80	0.62
16	0.75	0.58
AVERAGE	0.82	0.63

Table 6.1: Summary of the water released by each lysimeter during the period considered and ratio μ of the water released divided by the volume of precipitation corresponding to each section (1.29 m^3)

The periodogram of the rainfall is showed in Figure 6.2(a). The periodogram is flat indicating that the rainfall events have a short time correlation. Figure 6.2(b) shows the spectrum of the outflow through lysimeter 9 for comparing purposes. This section of the pile is acting as a low-pass filter attenuating the input signal at high frequencies. The residual energy of the signal at high frequencies is produced by a fast flow component (i.e. preferential flow) that results in an asymptotic behavior of the spectrum.

6.3.4 Conceptual model

The two components of flow (i.e. fast and slow) have been decoupled assuming that the rate of flow is different in the two zones of the domain (i.e. matrix and macropores). In our model we assume that there is no interchange between the two zones and that the water that infiltrates through the macropores is released instantaneously. Using spectral representation we can express

the water outflow in the basal lysimeters as follows

$$dZ_q(\omega) = (F_{matrix}(\omega)(1-\alpha)+\alpha)dZ_r(\omega) \tag{6.6}$$

where dZ_q and dZ_r are the spectral amplitudes of the outflow and the effective infiltration respectively, α is the fraction of the effective infiltration that is driven through the macropores and F_{matrix} is the spectral amplitude of the impulse response of the matrix.

If we take the expected value of dZ_q times its complex conjugate we can express the TF of the whole system as follows

$$|F_{whole}(\omega)|^2 = (F_{matr}(\omega)(1-\alpha)+\alpha))(F^*_{matr}(\omega)(1-\alpha)+\alpha)) \tag{6.7}$$

An explicit expression of (6.7) is obtained by considering the matrix as a linear reservoir [27]. In this case we can express the relationship between the effective infiltration and the outflow through the matrix as follows

$$\frac{dV(t)}{dt} = r_{matr}(t) - q_{matr}(t) \tag{6.8}$$

where $r_{matr} = (1-\alpha)r$ and q_{matr} are the effective infiltration and the outflow through the matrix, and V is the volumetric soil moisture given by

$$V(t) = \int_0^{z_0} \theta(z,t)dz \tag{6.9}$$

where θ is the local soil moisture content and z_0 is the vertical extent of the unsaturated zone in this case the full height of the rock pile. The outflow q_{matr} is related to V by

$$q_{matr}(t) = a_l(V(t) - V_0) \tag{6.10}$$

where a_l is the soil-moisture-reservoir coefficient and V_0 is the minimum soil-moisture storage approximately equal to the field capacity times the vertical extent of the unsaturated zone ($V_0 = \theta_0 z_0$).

It is worthwile to note that the soil-reservoir-coefficient has dimensions of inverse time unit ($\left[T^{-1}\right]$) and is somehow representative of the lag-time of the water released by the matrix. In other words, the inverse of the soil-reservoir-coefficient is a characteristic time which quantifies the velocity of dissipation of a perturbation taking place at the surface of an equivalent matrix reservoir.

By combining (6.8) and (6.10) and using spectral representation we can write F_{matr} as follows

$$F_{matr} = \frac{1 - i\omega/a_l}{1 + \omega^2/a_l^2} \tag{6.11}$$

By substituting F_{matr} and its complex conjugate into (6.7) we obtain an explicit expression of the TF of the system

$$|F_{whole}(\omega)|^2 = \frac{1}{1 + \Omega^2}(1 - \alpha^2) + \alpha^2 \tag{6.12}$$

where $\Omega = \omega/a_l$. From Figure 6.3 we see that, when there is no preferential flow ($\alpha = 0$), F_{whole} decreases linearly with the logarithm of the dimensionless frequency (Ω) meaning that at high frequencies the energy of the impulse response is almost null. As already observed in the previous section, in the presence of preferential flow, the transfer function shows an asymptotic behavior where the energy of the impulse response signal at high frequencies is proportional to the square of α.

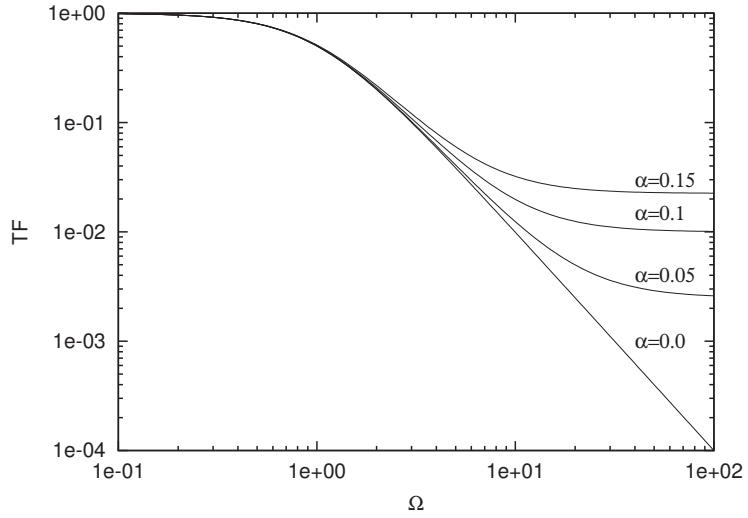

Figure 6.3: Dimensionless parametric TF as a function of different α values.

6.4 Results and discussion

As already stated in the previous chapters, the presence of preferential flow in a given section of the pile is directly reflected by the shape of the spectrum of its outflow time series. This means that a section where the flow is mainly driven by the matrix acts as a perfect low-pass filter while a section where an important fraction of the infiltration is channeled and released by the macropores has a spectrum showing an asymptotic behavior.

Figure 6.4(a) shows the spectrum of the outflow through lysimeter 8 and 9. Altough both lysimeters released almost the same quantity of water during the period considered (see Table 6.1), their spectral density functions are different at high frequencies where the energy of the output signal through lysimeter 8 is higher than that through lysimeter 9. This behavior is confirmed by looking at the outflow through both lysimeters after the application of a single artificial rainfall event on 18 July 2000 (Figure 6.4b). Lysimeter 8 shows a fast and sharp response to the artificial recharge while the outflow through lysimeter 9 is smooth showing a slow response.

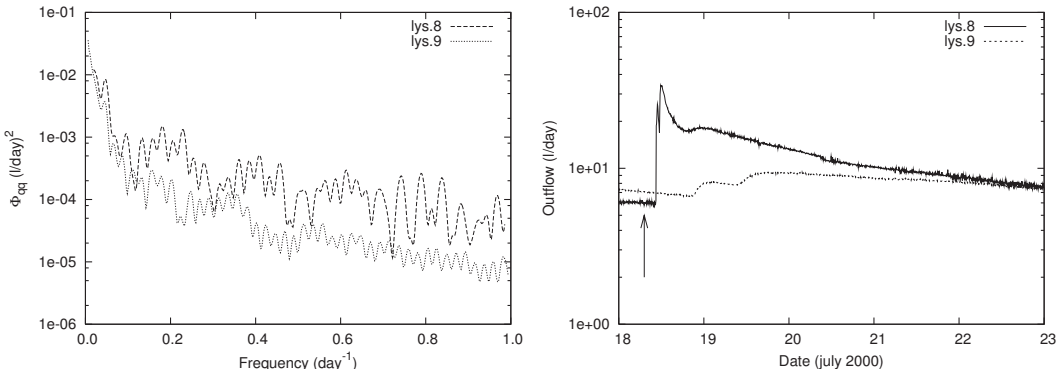

Figure 6.4: Periodogram of the outflow through lysimeter 8 and 9 (a) and outflow through the same lysimeter after the application of a single artificial rainfall event (indicated by the arrow) (b)

lysimeter	$a_1(day^{-1}$	α
1	0.02	0.03
2	0.02	<0.01
3	0.03	<0.01
4	0.03	<0.01
5	0.02	0.03
6	0.03	0.14
7	0.04	0.08
8	0.03	0.10
9	0.02	0.04
13	0.04	<0.01
14	0.03	<0.01
15	0.03	<0.01
16	0.04	0.05

Table 6.2: results of the calibration for each individual lysimeter

The empirical TF of each lysimeter has been computed following the methodology and the data treatment explained in the previous sections. Each empirical TF has been parametrized using Equation 6.12. The two fitting parameters (a_l and α) have been calibrated by a trial and error approach that minimizes the sum of squared differences between the empirical TF and the parametric TF. The results of the calibration are shown in Figure 6.5 and summarized in Table 6.2 for each lysimeter with the exception of lysimeters 10 11 and 12 that have a noisy time-series that makes the calibration unreliable.

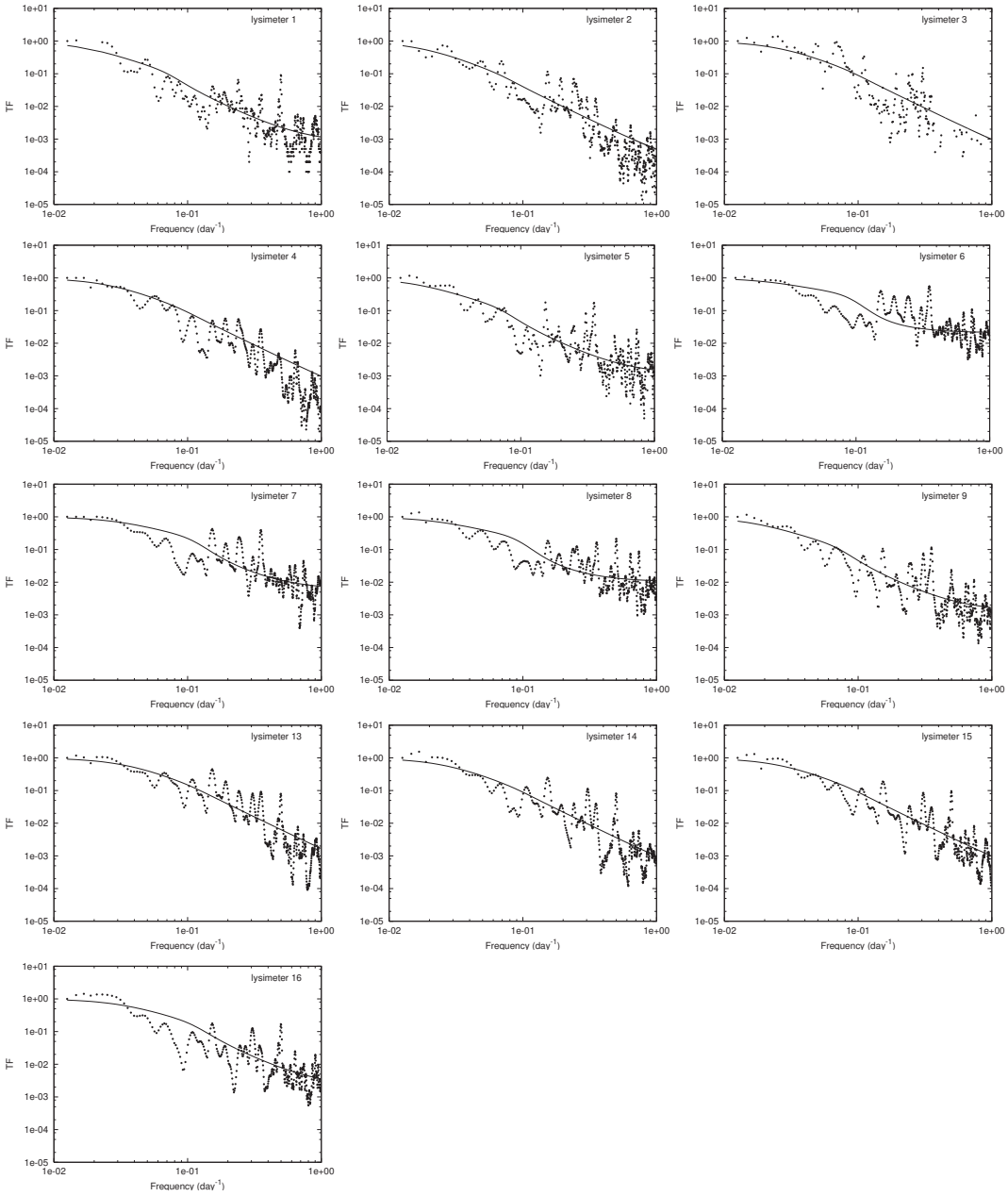

Figure 6.5: Empirical TF (dotted line) and simulated TF (solid line) for each lysimeter

From the table we can see that the soil-moisture-reservoir coefficient (a_l) is quite constant ranging from $0.02 day^{-1}$ to $0.04 day^{-1}$. The meaning of this parameter can be understood by looking at the solution of (6.8) that takes this form

$$V - V_0 = (V_s - V_0) \exp(-a_l t) \tag{6.13}$$

where V_s is the initial soil-moisture content averaged over the vertical extent of the unsaturated zone. By analogy with radioactive decay, we can define a characteristic time of the matrix in the following form

$$t_c = \frac{1}{a_l} \ln(2) \tag{6.14}$$

t_c represents the time when half of the perturbation (i.e. recharge) occurring at the top of an equivalent matrix system, is dissipated (i.e. released) at the bottom. The characteristic times obtained from the calibration range between 17 and 34 days. It is worthwhile to note that in our methodology we in effect homogenize the matrix by lumping its intrinsic heterogeneities within only one parameter (a_l). In the calibration process, a_l are strongly influenced by the fastest components of the discharge through the matrix while the very slow base discharge is implicitly neglected because of the time-series that we analyze is only 8 months in duration. This makes difficult to correlate the estimated characteristic time with the residence time calculated using the classical methodology of net infiltration divided by mean volumetric content times effective volume, or by travel time of a tracer through the system.

The calibrated α values show a high space variability. This occurs as a consequence of the direct dependence of preferential flow on the spatial arrangement of matrix-supported and matrix-free zones. In the study of *Nichol et al.* [70] local regions that are matrix-supported and local regions with matrix-free cobbles and boulders were observed during construction. From Table 6.2

we see that there is a set of lysimeters that has a very low fraction of preferential flow (lysimeters 2,3,4,13,14 and 15). This fraction is lower than 1% out of the total flow volume but an accurate estimation of this value is not possible because of the very low energy of the corresponding outflow time-series at high frequencies. Another set of lysimeters (lysimeter 1,5,9 and 16) shows a moderate rate of preferential flow ranging from 3% to 5% while the remaining lysimeters (lysimeter 6,7 and 8) show an important component of preferential flow ranging from 8 to 14%. It is interesting to note that the lysimeters belonging to each group are spatially clustered. This scale of clustering suggests heterogeneity larger than the largest boulder size and may be related to the construction technique or the random position of the very large ($> 0.5m$ diameter) boulders within the pile.

Figure 6.6 displays a scatter plot of the α value and the amount of water released by each lysimeter during the period considered. The points of the plot are quite dispersed indicating a poor correlation between the two variables. It is interesting to note that there are lysimeters that release a relatively large amount of water despite showing a limited presence of preferential flow (e.g. lysimeter 13) while others lysimeters are largely influenced by preferential flow but release a relatively small quantity of water.

lysimeters	α
SW(1+2+5+6)	0.07
NW(3+4+7+8)	0.04
SE(9+10+13+14)	0.01
NE(11+12+15+16)	0.02

Table 6.3: results of the calibration for a combination of four lysimeters aggregated (see Figure 6.7)

The same analysis that was carried out for individual lysimeters has also been performed on outflow data created by aggregating the outflow from contiguous lysimeters into quarters of the pile as indicated in Figure 6.7. The results of the calibration to these aggregated outflows are shown in Figure 6.8 and summarized in Table 6.3. The soil-reservoir coefficient has been considered constant equal to the arithmetic mean of the calibrated values of the individual lysimeters (a_l = 0.03). Quarters SW and NW have a calibrated α that is approximately equal to the mean of the α

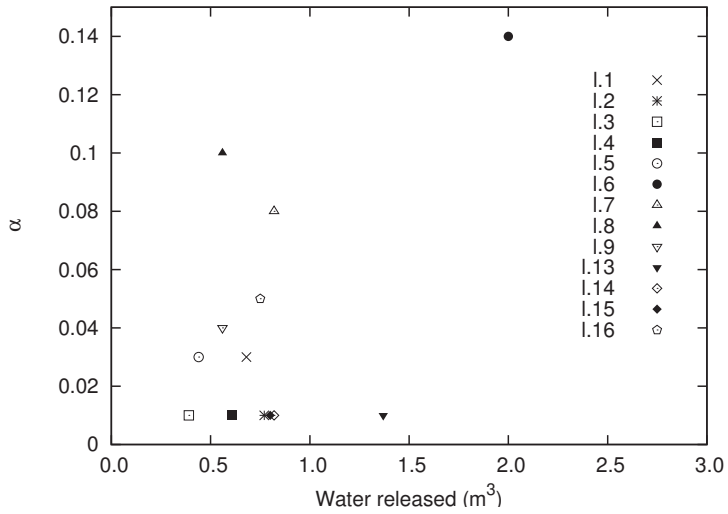

Figure 6.6: Water released during the period considered (March 1 - October 30, 2000) versus calibrated α

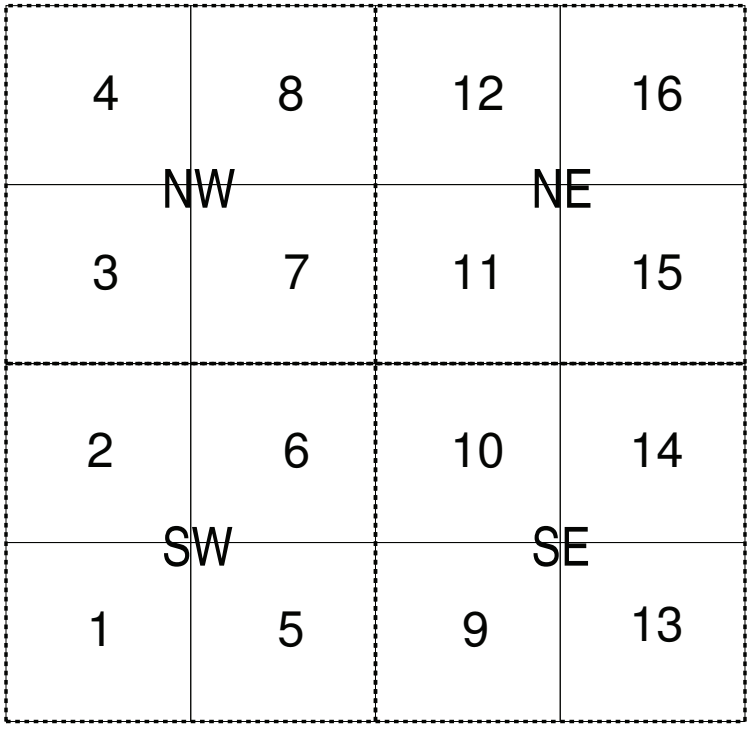

Figure 6.7: Location of the lysimeters aggregated into quartes

values of their individual lysimeters. An analogous reasoning cannot be made for the remaining two quarters since we lack of reliable calibrated values of lysimeter 10, 11 and 12 although it is evident that as the scale of the lysimeter increases the variability of α decreases. This observation is confirmed by a further 'upscaling' obtained by aggregating all the lysimeters together. The calibration of the resulting TF (Figure 6.9) gives an estimated α lower than 0.01 indicating that at large scales the pile is acting as an equivalent matrix reservoir.

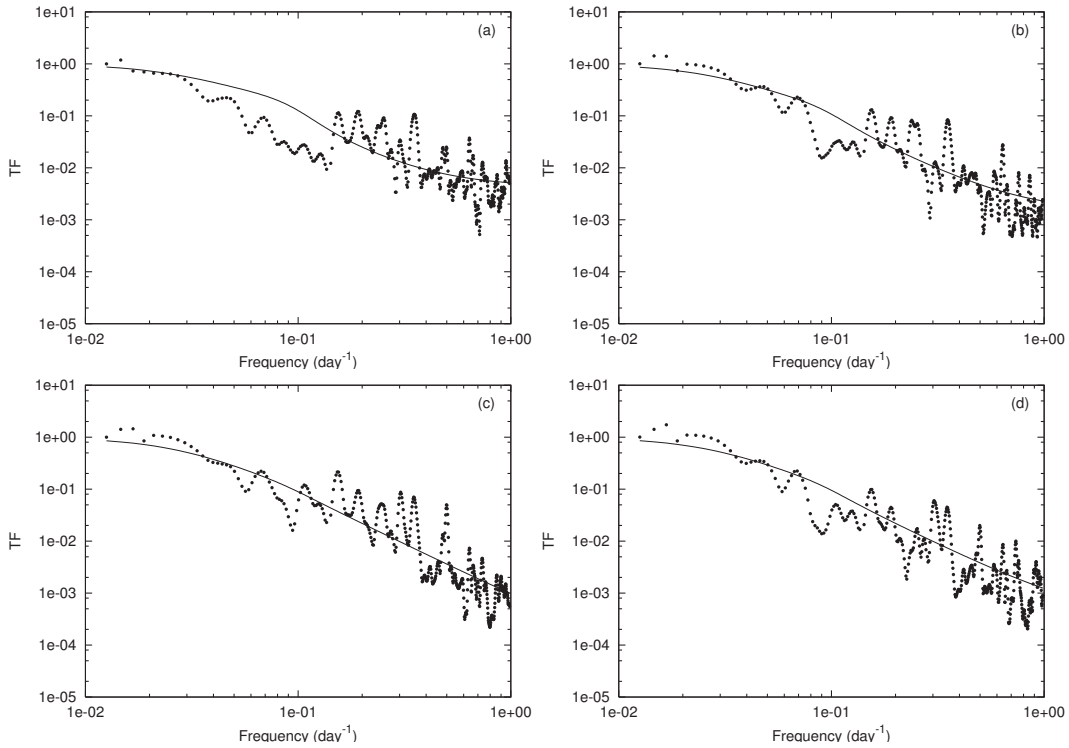

Figure 6.8: Empirical TF (dotted line) and simulated TF (solid line) for the qarters (a) SW, (b) NW, (c) SE and (d) NE.

6.5 Conclusions

We modelled unsaturated water flow through a highly heterogeneous unsaturated medium using a simple linear representation. Such a model cannot accurately describe the complexity of the

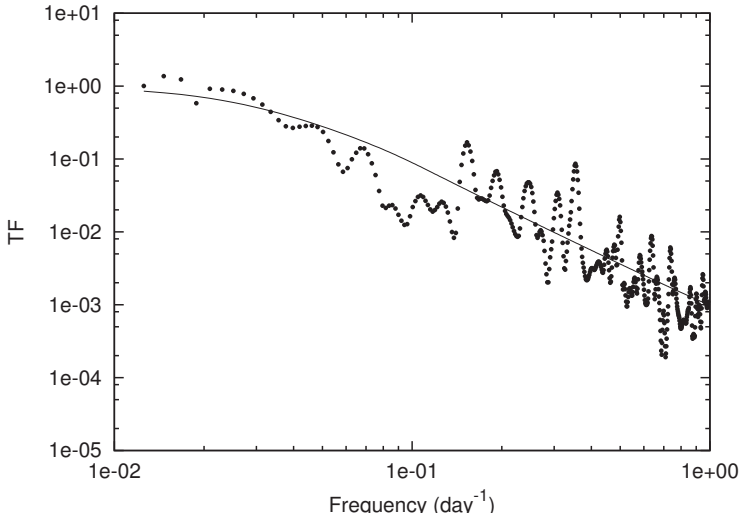

Figure 6.9: Empirical TF (dotted line) and simulated TF (solid line) of the all lysimeters aggregated into one.

medium at the local scale but is useful to obtain a first-order identification of the averaged processes occurring within it. The main advantage of this methodology lies in its simplicity that allows to infer information about the characteristic time of the hydraulic response of the matrix and the degree of preferential flow occurring within each section of the pile by looking at the spectral signature of the input and the output. The main conclusions of the study can be summarized as follows

1. The ratio between the amount of rainfall and the amount of water released by each lysimeter in the same period (March 1 to October 31, 2000) highlights the important role played by horizontal redistribution. This effect is implicitly taken into account by the model through the normalization coefficient μ (Equation 6.5).

2. The calibration of the model allows one to infer information about the characteristic time of the flow through the matrix (Equation 6.14). The results show that a_l is quite constant, being related to the textural properties of the matrix and not to the spatial arrangements of the well-structured soil. The characteristic time inferred does not account for the flow components slower

than the eight-month period of data analyzed.

3. The calibrated α values show a high space variability. The different degrees of preferential flow observed within each section of the pile are spatially clustered indicating a dependence of preferentail flow patterns with textural heterogeneities occurring as a result of the construction procedure.

4. A poor correlation is observed between the degree of preferential flow of a given section and the relative amount of water released by the same section.

5. If we repeat the calibration exercise considering larger sections of the pile (quarters, entire section) we see that the variability of α decreases and the behavior of the pile tends to approximate that of an equivalent matrix reservoir. This outcome is especially important in mining related problems. In fact at large scale the water pile is masking the effects of preferential flow leading to estimate of the residence time that can overestimate the (true) mean residence time of the water within the pile.

Chapter 7

Conclusions

In this chapter we summarize the main conclusions of this thesis.

The physical meaning of hydraulic parameters estimated using the assumption of aquifer homogeneity and the role played by heterogeneity in groundwater applications has been investigated. A number of frameworks have been provided to properly acount for heterogeneity and to obtain quantitative and semi-quantitative information of the underlying heterogeneous structure.

As already observed by *Meier et al.* [62] and *Sanchez-Vila et al.* [83], the storage coefficient estimated from pumping tests interpreted using the Cooper-Jacob method, S_{est}, is indicative of the flow point-to-point connectivity between the well and the observation point. Similarly, the porosity estimated from tracer tests interpreted using homogeneous isotropic medium, ϕ_{est}, is indicative of transport connectivity [29]. Our mathematical framework aims at giving insight into the weak correlation between the indicators of flow and transport connectivity already highlighted numerically by *Knudby and Carrera* [51]. Using a small perturbation approach we provided an approximated analytical solution that gives an explicit expression to ϕ_{est}. The resulting expression involves two terms. The first one depends on the transmissivity values located along the flow path line such that large transmissivity values, i.e., larger than the equivalent homogeneous transmissivity of the

aquifer, leads to estimates of ϕ_{est} smaller than ϕ (considered constant) and vice versa. The second term incorporates the hydraulic response of the aquifer (flow connectivity) induced by pumping, which is measured by the estimated storage coefficient, S_{est} defined by the observation point moving along the same path line. Point-to-point transport connectivity gets amplified/reduced when the time of the hydraulic response along the flow path line decreases/increases in the direction of flow.

The comparison of the analytical expression of S_{est} [83] and ϕ_{est} explains the weak correlation between the two indicators of connectivity. The indicator of flow connectivity, S_{est}, can be viewed as a weighted averaged over the entire domain, while the indicator of transport connectivity ϕ_{est} is a weighted averaged along the flow path line. Moreover, the transport weighting function (proportional to the radial distance) is remarkably different from that of flow connectivity, the latter assigning large weights to all the points located between the observation and the pumping well.

A proper identification of the connectivity patterns of an aquifer is important for a correct delineation of capture zones around a pumping well. Here the analytical framework has been extended to compute these connectivity patterns using a limited and sparse number of measurements. The lack of complete knowledge of the variables involved in the problem is overcome by treating them as regionalized variables. The methodology allows conditioning the results to three types of data measured over different scales, namely travel times of convergent tracer tests, t_a, estimates of the storage coefficient from pumping tests interpreted using the Cooper-Jacob method, S_{est}, and measurements of transmissivity point values, T.

The geostatistical framework has been tested using a synthetic field. The results show that when only a limited number of T measurements (16) is available, the predicted shape of the capture zone tends to that of an equivalent homogeneous field. In this scenario, the isoprobability contour lines obtained from 300 conditional simulations show a high uncertainty. The incorporation of tracer test data or the availability of more transmissivity measurements reduces the uncertainty improving the delineation of the protection area.

Another slightly different application that has been extensively studied in this thesis is the analysis of pumping tests in leaky aquifers. The development of a new methodology (DIP method) for the interpretation of this kind of hydraulic tests has been the starting point for the definition of a framework that allows to better understanding the physical meaning of the estimated parameters. Although the DIP method is based on the assumption of homogeneity, it allows obtaining two independent estimates that are based on different parts of the drawdown curve, thus providing indirect information about the heterogeneous distribution of the local transmissivity values.

A Monte Carlo approach has been used to give a framework that allows to better understanding the implications of the assumption of homogeneity in the estimates obtained with the different methods commonly used in the interpretation of pumping tests in aquifer-aquitard systems (Hantush inflection point method, Walton type-curve method and DIP method). Since each method give different emphasis to different portions of the drawdown curve and, consequently to different volumes of the aquifer-aquitard system, we conclude that using all analysis methods jointly may provide additional information (specifically, about contrasts in the local value of the transmissivty at the pumping well) than using each method independently. The study of the correlation functions between different transmissivity estimates and the value of transmissivity at the well confirms that methods based on the first part of the drawdown curve (DIP1, inflection point method) are indicative of the local transmissivity (nearby the well). The correlation tends to vanish with the distance from the well.

Additional degree of heterogeneity is observable in unsaturated flow conditions, especially in unstructured soils (e.g. waste rock piles) where the role of preferential flow is enhanced. In such media, the difficulty of implementation of mechanistic models (i.e. dual porosity models) arises from the need of a rigorous microscopic description of the medium to obtain reliable 'upscaled' hydraulic parameters and its application is usually limited to investigations purposes. In this thesis we propose a methodology to obtain first order identification of the averaged processes occurring within the medium (i.e. degree of preferential flow and some characteristic time of the

flow through the matrix) based on the study of the spectral signature of the input (net infiltration) and output (flow discharge). An application of the methodology at different scales suggests that at large scales the system behaves like an equivalent matrix system, thus masking the preferential flow and leading to estimate of the mean residence time that are larger than its actual value.

Bibliography

[1] Alcolea, A., E. Castro, M. Barbieri, J. Carrera, and S. Bea (2007), Inverse modeling of coastal aquifers using tidal response and hydraulic tests, *Ground Water*, *45*(6), 711–722.

[2] Amin, I. (2005), Determination of the rate and volume of leakage using the slopes of time-drawdown data, *Environmental Geology*, *47*(4), 558–564.

[3] Barker, J., and R. Herbert (1982), Pumping tests in patchy aquifers, *Ground Water*, *20*(2), 150–155.

[4] Bauters, T. W. J., D. A. DiCarlo, T. S. Steenhuis, and J. Y. Parlange (1998), Preferential flow in water-repellent sands, *Soil Science Society Of America Journal*, *62*(5), 1185–1190.

[5] Berkowitz, B. (1995), Analysis of fracture network connectivity using percolation theory, *Mathematical Geology*, *27*(4), 467–483.

[6] Beven, K., and P. Germann (1982), Macropores and water-flow in soils, *Water Resources Research*, *18*(5), 1311–1325.

[7] Boulton, N. (1954), The drawdown of the water table under nonsteady conditions near a pumped well in an unconfined formation: Proc, *Civil Engineers (British)*, pp. 564–579.

[8] Bour, O., and P. Davy (1997), Connectivity of random fault networks following a power law fault length distribution, *Water Resources Research*, *33*(7), 1567–1583.

[9] Bourdet, D. (2002), *Well test analysis: The use of advanced interpretation models*, 426 pp., Elsevier, Amsterdam.

[10] Bourdet, D., T. M. Whittle, A. A. Douglas, and Y. M. pirard (1983), A new set of type curves simplifies well test analysis, *World Oil*, *196*(6), 95–106.

[11] Butler, J. J. (1988), Pumping tests in nonuniform aquifersthe radially symmetric case, *Journal of Hydrology*, *101*(1-4), 15–30.

[12] Butler, J. J., and W. Z. Liu (1993), Pumping tests in nonuniform aquifersthe radially asymmetric case, *Water Resources Research*, *29*(2), 259–269.

[13] CIS (2007), Groundwater in drinking water protected areas - the implementation challenge of the water framework directive. common implementation strategy for the water framework directive,, *Tech. rep.*, Guidance Document No. 16, produced by Working Group C.

[14] Cole, B., and S. Silliman (1997), Capture zones for passive wells in heterogeneous unconfined aquifers, *Ground Water*, *35*(1), 92–98.

[15] Cooper, H., and C. Jacob (1946), A generalized graphical method for evaluating formation constants and summarizing well-field history, *Trans Am Geophys Union*, *27*(4), 526–534.

[16] Copty, N., and A. Findikakis (2004), Stochastic analysis of pumping test drawdown data in heterogeneous geologic formations, *J. Hydraul. Res.*, *42*, 59–67.

[17] Copty, N. K., and A. N. Findikakis (2004), Bayesian identification of the local transmissivity using time-drawdown data from pumping tests, *Water Resources Research*, *40*(12), W12,408.

[18] Copty, N. K., M. S. Sarioglu, and A. N. Findikakis (2006), Equivalent transmissivity of heterogeneous leaky aquifers for steady state radial flow, *Water Resources Research*, *42*(4), W04,416.

[19] Copty, N. K., P. Trinchero, X. Sanchez-Vila, M. Sarioglu, and A. Findikakis (2008 accepted for pubblication)), Influence of heterogeneity on the interpretation of pumping test data in semiconfined aquifers, *Water Resources Research*.

[20] Darcel, C., O. Bour, P. Davy, and J. R. de Dreuzy (2003), Connectivity properties of two-dimensional fracture networks with stochastic fractal correlation, *Water resources research*, *39*(10), 1272.

[21] de Marsily, G. (1985), Flow and transport in fractured rocks: connectivity and scale effect, *Invited paper. International symposium on the hydrogeology of rocks of low permeability, Tucson AZ (USA), January*.

[22] deGlee, G. (1930), Over grondwaterstroomingen bij wateronttrekking door middel van putten, Ph.D. thesis, Delft Technische Hoogeschool.

[23] Dekker, L. W., and C. J. Ritsema (1996), Preferential flow paths in a water repellent clay soil with grass cover, *Water Resources Research*, *32*(5), 1239–1249.

[24] Denic-Jukic, V., and D. Jukic (2003), Composite transfer functions for karst aquifers, *Journal Of Hydrology*, *274*(1-4), 80–94.

[25] Desbarats, A. J. (1992), Spatial averaging of transmissivity in heterogeneous fields with flow toward a well, *Water Resources Research*, *28*(3), 757–767.

[26] Dreiss, S. J. (1983), Linear unit-response functions as indicators of recharge areas for large karst springs, *Journal Of Hydrology*, *61*(1-3), 31–44.

[27] Duffy, C. J., L. W. Gelhar, and P. J. Wierenga (1984), Stochastic-models in agricultural watersheds, *Journal Of Hydrology*, *69*(1-4), 145–162.

[28] Edwards, W. M., M. J. Shipitalo, L. B. Owens, and L. D. Norton (1989), Water and nitrate movement in earthworm burrows within long-term no-till cornfields, *Journal Of Soil And Water Conservation*, *44*(3), 240–243.

[29] Fernandez-Garcia, D., X. Sanchez-Vila, and T. H. Illangasekare (2002), Convergent-flow tracer tests in heterogeneous media: combined experimental-numerical analysis for determination of equivalent transport parameters, *Journal Of Contaminant Hydrology*, *57*(1-2), 129–145.

[30] Fernandez-Garcia, D., T. H. Illangasekare, and H. Rajaram (2005), Differences in the scale dependence of dispersivity and retardation factors estimated from forced-gradient and uniform flow tracer tests in three- dimensional physically and chemically heterogeneous porous mediaart. no. w03012, *Water Resources Research*, *41*(3), 3012–3012.

[31] Flury, M., H. Fluhler, W. A. Jury, and J. Leuenberger (1994), Susceptibility of soils to preferential flow of water - a field-study, *Water Resources Research*, *30*(7), 1945–1954.

[32] Fogg, G. (1986), Groundwater flow and sand body interconnectedness in a thick, multiple-aquifer system, *Water Resources Research*, *22*(5), 679–694.

[33] Fogg, G., S. Carle, and C. Green (2000), Connected-network paradigm for the alluvial aquifer system, *Special paper- Geological Society of America*, (348), 25–42.

[34] Gelhar, L. W., and C. L. Axness (1983), 3-dimensional stochastic-analysis of macrodispersion in aquifers, *Water Resources Research*, *19*(1), 161–180.

[35] Gerke, H., and M. van Genuchten (1993), A dual-porosity model for simulating the preferential movement of water and solutes in structured porous media, *Water Resour. Res*, *29*(1), 305–319.

[36] Gerke, H. H. (2006), Preferential flow descriptions for structured soils, *Journal Of Plant Nutrition And Soil Science-Zeitschrift Fur Pflanzenernahrung Und Bodenkunde*, *169*(3), 382–400.

[37] Gish, T. J., and W. A. Jury (1983), Effect of plant-roots and root channels on solute transport, *Transactions Of The Asae*, *26*(2), 440–&.

[38] Gomez-Hernandez, J., and X. Wen (1998), To be or not to be multi-gaussian? a reflection on stochastic hydrogeology, *Advances in Water Resources*, *21*(1), 47–61.

[39] Gringarten, A. (1971), Unsteady-state pressure distributions created by a well with a single horizontal fracture, partial penetration, or restricted entry, Ph.D. thesis, Stanford Univ., Stanford, CA.

[40] Guadagnini, A., and S. Franzetti (1999), Time-related capture zones for contaminants in randomly heterogeneous formations, *Ground Water*, *37*(2), 253–260.

[41] Guimera, J., and J. Carrera (2000), A comparison of hydraulic and transport parameters measured in low-permeability fractured media, *Journal Of Contaminant Hydrology*, *41*(3-4), 261–281.

[42] Hantush, M. (1956), Analysis of data from pumping tests in leaky aquifers, *Trans Am Geophys Union*, *37*(6), 702–14.

[43] Hantush, M. (1961), Drawdown around a partially penetrating well, in *Journal of Hydraulics Division, Proceedings of the American Society of Civil Engineers*, vol. 87, pp. 83–98.

[44] Hantush, M., and C. Jacob (1955), Non-steady radial flow in an infinite leaky aquifer, *Trans Am Geophys Union*, *36*(1), 95–100.

[45] Hantush, M. S. (1960), Modification of the theory of leaky aquifers, *Journal of Geophysical Research*, *65*(5), 1634–1634.

[46] Harbaugh, A., E. Banta, M. Hill, and M. McDonald (2000), Modflow-2000 the us geological survey modular ground-water model-user guide to modularization concepts and the ground-water flow process, *US Geological Survey Open-File Report 00-92*, *121*.

[47] Hill, D. E., and J. Y. Parlange (1972), Wetting front instability in layered soils, *Soil Science Society Of America Proceedings*, *36*(5), 697–&.

[48] Horne, R. (1995), *Modern Well Test Analysis: A Computer-aided Approach*, 257 pp., 2nd edn. Petroway, Inc., Palo Alto.

[49] Jacob, C. (1947), Drawdown test to determine effective radius of artesian well, *Transactions of the American Society of Civil Engineers*, *112*, 1047–1064.

[50] Kerrou, J., P. Renard, H. J. H. Franssen, and I. Lunati (2008), Issues in characterizing heterogeneity and connectivity in non-multigaussian media, *Advances In Water Resources*, *31*, 147–159.

[51] Knudby, C., and J. Carrera (2005), On the relationship between indicators of geostatistical, flow and transport connectivity, *Advances In Water Resources*, *28*(4), 405–421.

[52] Knudby, C., and J. Carrera (2006), On the use of apparent hydraulic diffusivity as an indicator of connectivity, *Journal Of Hydrology*, *329*(3-4), 377–389.

[53] Krishnan, S., and A. G. Journel (2003), Spatial connectivity: From variograms to multiple-point measures, *Mathematical Geology*, *35*(8), 915–925.

[54] Kung, K. (1990), Preferential Flow in a Sandy Vadose Zone: 1. Field Observation, *Geoderma,*, *46*, 51–58.

[55] Kung, K. (1990), Preferential Flow in a Sandy Vadose Zone: 2. Mechanism and Implications, *Geoderma,*, *46*, 59–71.

[56] LaBolle, E. M., and G. E. Fogg (2001), Role of molecular diffusion in contaminant migration and recovery in an alluvial aquifer system, *Transport In Porous Media*, *42*(1-2), 155–179.

[57] Liu, G. S., C. M. Zheng, and S. M. Gorelick (2007), Evaluation of the applicability of the dual-domain mass transfer model in porous media containing connected high-conductivity channels, *Water Resources Research*, *43*.

[58] Lomb, N. R. (1976), Least-squares frequency-analysis of unequally spaced data, *Astrophysics And Space Science*, *39*(2), 447–462.

[59] Long, A. J., and R. G. Derickson (1999), Linear systems analysis in a karst aquifer, *Journal Of Hydrology*, *219*(3-4), 206–217.

[60] Mantoglou, A., and J. l. Wilson (1982), The turning bands method for simulation of random-fields using line generation by a spectral method, *Water Resources Research*, *18*(5), 1379–1394.

[61] Manzocchi, T. (2002), The connectivity of two-dimensional networks of spatially correlated fractures, *Water Resources Research*, *38*(9), 1162.

[62] Meier, P. M., J. Carrera, and X. Sanchez-Vila (1998), An evaluation of jacob's method for the interpretation of pumping tests in heterogeneous formations, *Water Resources Research*, *34*(5), 1011–1025.

[63] Moench, A. (1985), Transient flow to a large-diameter well in an aquifer with storative semiconfining layers, *Water Resources Research*, *21*(8), 1121–1131.

[64] Molenat, J., P. Davy, C. Gascuel-Odoux, and P. Durand (1999), Study of three subsurface hydrologic systems based on spectral and cross-spectral analysis of time series, *Journal Of Hydrology*, *222*(1-4), 152–164.

[65] Nativ, R., E. Adar, O. Dahan, and M. Geyh (1995), Water recharge and solute transport through the vadose zone of fractured chalk under desert conditions, *Water Resources Research*, *31*(2), 253–261.

[66] Neuman, S., A. Guadagnini, and M. Riva (2004), Type-curve estimation of statistical heterogeneity, *Water Resources Research*, *40*(4), W04,201.

[67] Neuman, S., A. Blattstein, M. Riva, D. Tartakovsky, A. Guadagnini, and T. Ptak (2007),

Type curve interpretation of late-time pumping test data in randomly heterogeneous aquifers, *Water Resources Research*, *43*(10), 10,421.

[68] Neuman, S. P., and P. Witherspoon (1969), Theory of flow in a confined 2 aquifer system, *Water Resources Research*, *5*(4), 803–816.

[69] Neuman, S. P., and P. Witherspoon (1969), Applicability of current theories of flow in leaky aquifers, *Water Resources Research*, *5*(4), 817–829.

[70] Nichol, C., L. Smith, and R. Beckie (2005), Field-scale experiments of unsaturated flow and solute transport in a heterogeneous porous medium, *Water Resources Research*, *41*(5).

[71] Nicholl, M. J., R. J. Glass, and S. W. Wheatcraft (1994), Gravity-driven infiltration instability in initially dry nonhorizontal fractures, *Water Resources Research*, *30*(9), 2533–2546.

[72] Odling, N. E. (1997), Scaling and connectivity of joint systems in sandstones from western norway, *Journal Of Structural Geology*, *19*(10), 1257–1271.

[73] Papadopulos, I., and H. Cooper (1967), Drawdown in a well of large diameter, *Water Resources Res*, *3*, 241–244.

[74] Poeter, E., and P. Townsend (1994), Assessment of critical flow path for improved remediation management, *Ground Water*, *32*(3), 439–447.

[75] Priestley, M. (1981), *Spectral Analysis and Time Series, Volume 1: Univariate Series, Volume 2: Multivariate Series, Prediction and Control*, Probability and Mathematical Statistics.

[76] Ritsema, C. J., L. W. Dekker, J. M. H. Hendrickx, and W. Hamminga (1993), Preferential flow mechanism in a water repellent sandy soil, *Water Resources Research*, *29*(7), 2183–2193.

[77] Riva, M., L. Guadagnini, A. Guadagnini, T. Ptak, and E. Martac (2006), Probabilistic study of well capture zones distribution at the lauswiesen field site, *Journal Of Contaminant Hydrology*, *88*(1-2), 92–118.

[78] Roth, K., W. A. Jury, H. Fluhler, and W. Attinger (1991), Transport of chloride through an unsaturated field soil, *Water Resources Research*, *27*(10), 2533–2541.

[79] Rubin, Y. (2003), *Applied Stochastic Hydrogeology*, Oxford University Press, USA.

[80] Sanchez-Vila, X., and J. Carrera (1997), Directional effects on convergent flow tracer tests, *Mathematical geology*, *29*(4), 551–569.

[81] Sanchez-Vila, X., and Y. Rubin (2003), Travel time moments for sorbing solutes in heterogeneous domains under nonuniform flow conditions, *Water Resources Research*, *39*(4).

[82] Sanchez-Vila, X., J. Carrera, and J. Girardi (1996), Scale effects in transmissivity, *Journal of Hydrology*, *183*(1), 1–22.

[83] Sanchez-Vila, X., P. M. Meier, and J. Carrera (1999), Pumping tests in heterogeneous aquifers: An analytical study of what can be obtained from their interpretation using jacob's method, *Water Resources Research*, *35*(4), 943–952.

[84] Sanchez-Vila, X., A. Guadagnini, and J. Carrera (2006), Representative hydraulic conductivities in saturated groundwater flow, *Reviews of Geophysics*, *44*(3), RG3002.

[85] Schad, H., and G. Teutsch (1994), Effects of the investigation scale on pumping test-results in heterogeneous porous aquifers, *Journal Of Hydrology*, *159*(1-4), 61–77.

[86] Shafer, J. M. (1987), Reverse pathline calculation of time-related capture zones in nonuniform flow, *Ground Water*, *25*(3), 283–289.

[87] Simunek, J., N. J. Jarvis, M. T. van Genuchten, and A. Gardenas (2003), Review and comparison of models for describing non-equilibrium and preferential flow and transport in the vadose zone, *Journal Of Hydrology*, *272*(1-4), 14–35.

[88] Smith, L., and R. Beckie (2003), Hydrologic and geochemical transport processes in mine waste rock, *Environmental Aspects Of Mine Wastes*, *31*, 51–72.

[89] Strebelle, S. (2002), Conditional simulation of complex geological structures using multiple-point statistics, *Mathematical Geology*, *34*(1), 1–21.

[90] Theis, C. (1941), The effect of a well on the flow of a nearby stream, *Am. Geophys Union*, *22*, 734–738.

[91] Theis, C., G. Branch, and G. Survey (1952), *The Relation Between the Lowering of the Piezometric Surface and the Rate and Duration of Discharge of a Well Using Ground Water Storage*, US Dept. of the Interior, Geological Survey, Water Resources Division, Ground Water Branch.

[92] Thiem, G. (1906), *Hydrologische Methoden (Hydrological methods)*, Gebhardt.

[93] Trinchero, P., X. Sanchez-Vila, N. Copty, and A. Findikakis (2008), A new method for the interpretation of pumping tests in leaky aquifers, *Ground Water*, *46*(1), 133–143.

[94] Trinchero, P., X. Sanchez-Vila, and D. Fernandez-Garcia (2008), Point-to-point connectivity, an abstract concept or a key issue for risk assessment studies?, *Advances in Water Resources*, *10.1016/j.advwatres.2008.09.001*.

[95] van Everdingen, A. (1953), The skin effect and its influence on the productivity capacity of a well, *Petrol Trans, AIME*, *198*, 171–176.

[96] van Genuchten, M., and P. Wierenga (1976), Mass Transfer Studies in Sorbing Porous Media I. Analytical Solutions, *Soil Science Society of America Journal*, *40*(4), 473.

[97] Varljen, M. D., and J. M. Shafer (1991), Assessment of uncertainty in time-related capture zones using conditional simulation of hydraulic conductivity, *Ground Water*, *29*(5), 737–748.

[98] Varni, M., and J. Carrera (1998), Simulation of groundwater age distributions, *Water Resources Research*, *34*(12), 3271–3281.

[99] Walton, W. (1962), *Selected analytical methods for well and aquifer evaluation*, Illinois State Water Survey.

[100] Western, A. W., G. Bloschl, and R. B. Grayson (2001), Toward capturing hydrologically significant connectivity in spatial patterns, *Water Resources Research*, *37*(1), 83–97.

[101] Willmann, M., J. Carrera, and X. Sanchez-Vila (2007), Transport upscaling: Effects of heterogeneity on memory functions, *Water Resources Research (Submitted)*.

[102] Yeh, T. C. J., and S. Y. Liu (2000), Hydraulic tomography: Development of a new aquifer test method, *Water Resources Research*, *36*(8), 2095–2105.

[103] Zheng, C. M., and S. M. Gorelick (2003), Analysis of solute transport in flow fields influenced by preferential flowpaths at the decimeter scale, *Ground Water*, *41*(2), 142–155.

[104] Zhu, J. F., and T. C. J. Yeh (2005), Characterization of aquifer heterogeneity using transient hydraulic tomography, *Water Resources Research*, *41*(7).

[105] Zinn, B., and C. F. Harvey (2003), When good statistical models of aquifer heterogeneity go bad: A comparison of flow, dispersion, and mass transfer in connected and multivariate gaussian hydraulic conductivity fields, *Water Resources Research*, *39*(3), 1051.